

Multi-neutron transfer in ^8He -induced reactions near the Coulomb barrierI. Martel **Department of Physics, University of Liverpool, Liverpool L69 9ZE, United Kingdom*

N. Keeley

*National Centre for Nuclear Research, ul. Andrzeja Soltana 7, 05-400 Otwock, Poland*K. W. Kemper †*Department of Physics, The Florida State University, Tallahassee, Florida 32306, USA*K. Rusek *Heavy Ion Laboratory, University of Warsaw, ul. Pasteura 5A, 02-093 Warsaw, Poland*

(Received 30 April 2020; revised 29 June 2020; accepted 17 August 2020; published 10 September 2020)

The measured inclusive ^6He and ^4He production cross sections of Marquínez-Durán *et al.*, [Phys. Rev. C **98**, 034615 (2018)] are reexamined and the conclusions concerning the relative importance of $1n$ and $2n$ transfer to the production of ^6He arising from the interaction of a 22 MeV ^8He beam with a ^{208}Pb target revised. A consideration of the kinematics of the $2n$ -stripping reaction when compared with the measured ^6He total energy versus angle spectrum places strict limits on the allowed excitation energy of the ^{210}Pb residual, constraining distorted wave Born approximation calculations such that the contribution of the $2n$ stripping process to the inclusive ^6He production can only be relatively small. It is therefore concluded that the dominant ^6He production mechanism must be $1n$ stripping followed by decay of the ^7He ejectile. Based on this result we present strong arguments in favor of direct, one-step four-neutron ($4n$) stripping as the main mechanism for ^4He production.

DOI: [10.1103/PhysRevC.102.034609](https://doi.org/10.1103/PhysRevC.102.034609)**I. INTRODUCTION**

The existence of multi-neutron clustering in nuclei has attracted considerable attention in recent years. The simplest such cluster, the dineutron, is unbound but a dominant dineutron contribution to the ^6He ground state has been well established both theoretically [1] and experimentally [2]. With a probable structure of an α core surrounded by four “valence” neutrons, ^8He provides the interesting additional possibility of $3n$ and $4n$ clustering as well as $2n$, and early studies of the $^{64}\text{Ni}(^4\text{He}, ^8\text{He})^{60}\text{Ni}$ [3] reaction suggested the presence of a strong one-step process, which could be well described as transfer of a $4n$ cluster. However, Wolski *et al.* [4], investigating elastic scattering of ^8He from ^4He , observed enhancement of the differential cross section at backward scattering angles that could be attributed to the sequential transfer of neutron pairs from the ^8He ground state.

The very complete study by Lemasson *et al.* [5] of the direct reactions induced by ^8He on ^{65}Cu at Coulomb barrier energies showed the dominance of neutron-transfer reactions, suggesting the existence of important correlations among the

valence neutrons in the ^8He ground state. More recently, Marquínez-Durán *et al.* [6] studied the scattering of ^8He from the doubly magic nucleus ^{208}Pb at 16 and 22 MeV and, in addition to the elastic scattering, the energy distributions and cross sections for ^6He and ^4He events were obtained. The energy distribution of the ^6He events clearly pointed to the presence of two production mechanisms, one- and two-neutron transfer reactions. On the other hand, the energy distribution of the α particles suggested the presence of three- and four-neutron stripping mechanisms.

The five-body ($\alpha + n + n + n + n$) cluster orbital shell model approximation (COSMA) calculations of the ^8He ground state by Zhukov *et al.* [7] seem to bear out these conclusions, since of the three configurations of the four valence neutrons with maximum probability one resembles a $4n$ cluster and one a pair of $2n$ clusters (or possibly a more loosely correlated $4n$ cluster). The third configuration corresponds to a more spatially symmetrical arrangement of the four neutrons around the α core. Thus, transfers of $2n$ and $4n$ clusters as well as single neutron transfer should be possible according to this model.

In this work we reexamine the inclusive ^6He and ^4He production data of Ref. [6] and revise our previous conclusion that at an incident ^8He energy of 22 MeV the $^{208}\text{Pb}(^8\text{He}, ^7\text{He})^{209}\text{Pb}$ single-neutron stripping reaction contributes approximately one third ($33 \pm 7\%$) of the measured inclusive ^6He cross section, with the remaining two thirds

*Present address: Department of Integrated Sciences, University of Huelva, 21071 Huelva, Spain; imartel@uhu.es

†Heavy Ion Laboratory, University of Warsaw, ul. Pasteura 5A, 02-093 Warsaw, Poland.

almost exclusively due to the $^{208}\text{Pb}(^8\text{He}, ^6\text{He})^{210}\text{Pb}$ two-neutron stripping reaction. A more detailed consideration of the reaction kinematics in connection with the experimental two-dimensional ^6He total energy versus scattering angle spectrum places strict limits on the allowed excitation energy range of the states in the ^{210}Pb residual that may be populated via the two-neutron stripping reaction. Distorted wave Born approximation (DWBA) calculations of the two-neutron stripping process consistent with these limits are unable to reproduce the shape of the measured inclusive ^6He angular distribution, forcing the conclusion that direct two-neutron stripping can make only a relatively minor contribution to the observed ^6He yield (of the order of 16% of the total cross section). The small magnitude of the initial $2n$ -stripping step in turn rules out sequential $2n$ - $2n$ transfer—the $^{208}\text{Pb}(^8\text{He}, ^6\text{He}), (^6\text{He}, ^4\text{He})^{212}\text{Pb}$ process—as a significant source of ^4He production. Since this is the most likely sequential route, we therefore argue that the ^4He production is dominated by direct $4n$ stripping. The good description of the measured inclusive ^4He angular distribution by DWBA calculations is consistent with this assumption.

II. ANALYSIS OF THE ^6He AND ^4He YIELDS

The inclusive ^6He and ^4He yields of Ref. [6] were measured simultaneously with the elastic scattering at the SPIRAL facility of the GANIL laboratory in France using the double-sided silicon strip detector array GLORIA [8]. Thanks to the excellent optical properties of the ^8He beam, together with an on-target intensity of 10^5 pps, an elastic scattering angular distribution of comparable quality to the best stable beam data was obtained, the different He isotopes being clearly separated in the detectors. In this work we confine our attention to the ^6He and ^4He data at 22 MeV since these have better statistical accuracy and clearly defined peaks in the angular distributions, thus providing more severe constraints on their interpretation. The angular distributions for ^6He and ^4He production [6] were obtained from the respective energy vs angle plots after selecting the corresponding isotope in the particle identification spectrum. Breakup and fusion-evaporation contributions were largely excluded by a careful consideration of the kinematics. Therefore, in the angular regions examined in this study there should only be a background contribution from processes other than neutron transfer, adequately described with an exponential function. See Refs. [6,8,9] for further details of the experimental setup and data reduction procedures.

A. Analysis of the ^6He yield

Before discussing the origin of the ^4He production we consider that of ^6He in detail. The measured ^6He yield [6] could result from the following four processes:

- (1) $^{208}\text{Pb}(^8\text{He}, ^7\text{He} + n \rightarrow ^6\text{He} + n + n)^{208}\text{Pb}$ ($1n$ breakup).
- (2) $^{208}\text{Pb}(^8\text{He}, ^6\text{He} + 2n)^{208}\text{Pb}$ ($2n$ breakup).
- (3) $^{208}\text{Pb}(^8\text{He}, ^7\text{He} \rightarrow ^6\text{He} + n)^{209}\text{Pb}$ ($1n$ transfer).
- (4) $^{208}\text{Pb}(^8\text{He}, ^6\text{He})^{210}\text{Pb}$ ($2n$ transfer).

In Ref. [6] we adduced arguments in favor of breakup processes providing an essentially negligible contribution to the inclusive ^6He yield in the angular range considered; there may be some small “background” from these reactions that falls off approximately exponentially with scattering angle. This leaves us with $1n$ and $2n$ transfer reactions. It is possible to assess the relative $1n$ and $2n$ contributions via DWBA calculations since these can show the kinematic differences between the two reactions. The one-neutron transfer has an optimum Q value of around -0.4 MeV, leading to population of low-lying bound states of ^{209}Pb with well known spectroscopic factors, thus enabling quantitative DWBA calculations. Since the entrance channel elastic scattering was also measured, in principle the only unknown is the exit channel $^7\text{He} + ^{209}\text{Pb}$ distorting potential. For the $2n$ cluster transfer, the optimum Q value is -0.8 MeV [6]. This reaction should therefore in principle preferentially populate excited states of ^{210}Pb at energies around $E_x = 8$ MeV, very close to the two-neutron binding energy ($S_{2n} = 9.1$ MeV), in good agreement with the measured ^6He energy spectrum [6]. At this high excitation energy the structure of ^{210}Pb is not known so that only qualitative DWBA calculations can be performed. However, the range of allowed excitation energies of the ^{210}Pb residual can be fixed from the observed two-dimensional ^6He total energy versus scattering angle spectrum purely by kinematics.

Figure 1 (a) clearly shows that if we assume direct $2n$ stripping as the ^6He production mechanism then only states in ^{210}Pb with excitation energies in the range $7 \leq E_x \leq 13$ MeV can be populated, with $E_x \approx 10$ MeV, slightly larger than that corresponding to the calculated Q_{opt} value, being most likely.

We therefore performed DWBA calculations of the $^{208}\text{Pb}(^8\text{He}, ^6\text{He})^{210}\text{Pb}$ reaction subject to these constraints in order to ascertain the angular position of the peak of the predicted ^6He angular distribution for comparison with the measured inclusive ^6He angular distribution at 22 MeV [6]. All DWBA calculations were performed with the code FRESKO [10]. The entrance channel potential used the same parameters as in Ref. [6] and the exit channel $^6\text{He} + ^{210}\text{Pb}$ potential used the 22 MeV parameters of Ref. [11]. The bound state potentials for the $2n$ cluster bound to the ^6He and ^{208}Pb cores were of standard Woods-Saxon form, with $r_0 = 1.38 \times A_{\text{core}}^{1/3}$ fm and $a = 0.7$ fm for the $(^8\text{He} | ^6\text{He} + 2n)$ overlap [12] and $r_0 = 1.25 \times A_{\text{core}}^{1/3}$ fm and $a = 0.7$ fm for the $(^{210}\text{Pb} | ^{208}\text{Pb} + 2n)$. The $2n$ cluster was assumed to have spin-parity 0^+ . Since these calculations were purely qualitative the spectroscopic factors for both overlaps were set to 1.0.

Calculations were performed for transfers leading to states in ^{210}Pb at excitation energies of $E_x = 7, 10,$ and 13 MeV, covering the kinematically allowed range, and several values of the transferred angular momentum L for each E_x . The dotted curve in Fig. 1(b) denotes the result of the DWBA $2n$ -stripping calculation for $E_x = 10$ MeV and $L = 4\hbar$, approximately the best matched L value. The shape of the calculated angular distribution does not reproduce the measured one and it peaks at $\theta_{\text{lab}} \approx 84^\circ$, about 10° larger than the measured ^6He angular distribution. While the detailed shape of the calculated angular distribution depends slightly on L and the choice of exit channel optical potential, the position of the peak is essentially

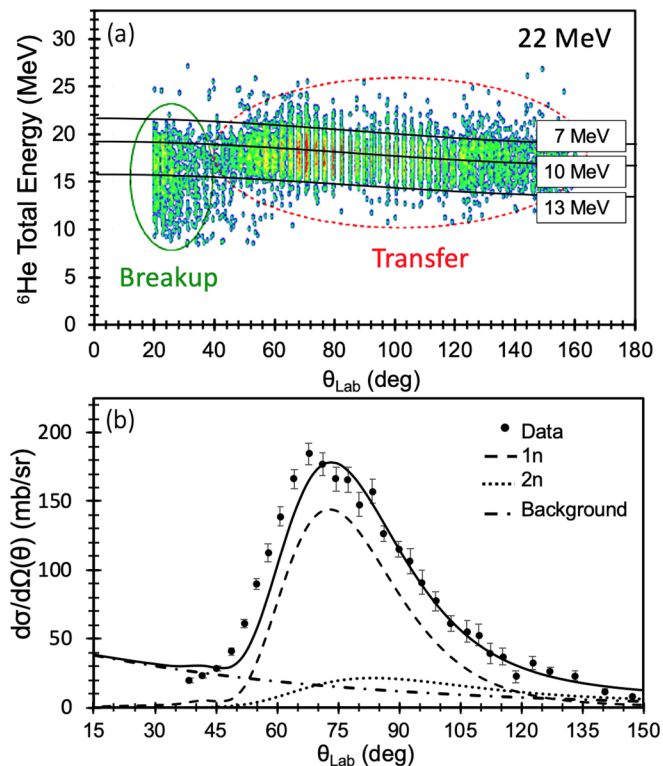


FIG. 1. (a) Experimental ^6He total energy versus scattering angle two-dimensional spectrum for 22 MeV ^8He incident on a ^{208}Pb target. Superimposed are kinematic curves for ^6He ejectiles produced by the $^{208}\text{Pb}(^8\text{He}, ^6\text{He})^{210}\text{Pb}$ $2n$ -stripping reaction with the ^{210}Pb residual in states with $E_x = 7, 10,$ and 13 MeV (reading from the top down). (b) Angular distribution of the differential cross section for inclusive ^6He production at $E_{\text{lab}} = 22$ MeV. The curves correspond to the different contributions: dashed curve - one neutron transfer, dotted curve - $2n$ cluster transfer, dot-dashed curve - background, and solid curve - total. See text for details.

fixed by kinematics, i.e., the value of E_x , with variations due to different input choices being of the order of 3° at most. The exit channel $^6\text{He} + ^{210}\text{Pb}$ optical potentials are rather well determined since the relevant incident energy range is covered by the $^6\text{He} + ^{208}\text{Pb}$ potentials of Ref. [11], which should not differ significantly from those for a ^{210}Pb target. If α -particle optical potentials are used instead in the exit channel—a rather extreme assumption—the stripping peak is shifted by about 3° to larger angles, i.e., making the description of the data worse. This relative insensitivity to the choice of exit channel optical potential is to be expected since the energies of the ^6He recoils when populating the levels of ^{210}Pb concerned are at or below the relevant Coulomb barrier. Reducing E_x by a few MeV moves the peak cross section to more forward angles but it is clear from Fig. 1(a) that the $2n$ -stripping cross section for such values of E_x must be negligible, since little or no ^6He are observed with the required energy. The shape is also not improved. We therefore arrive at the inescapable conclusion that direct $2n$ stripping can only make a minor contribution to the ^6He production *on kinematical grounds alone*, since no variation of the input parameters will enable the shape of the measured angular distribution to be reproduced by DWBA

calculations if E_x remains within the kinematically allowed limits.

Since we argue elsewhere [6] that breakup will only make a small contribution to the ^6He yield in the angular region considered here, essentially constituting an approximately exponentially falling background, this leaves one-neutron stripping as the main ^6He production process. The one neutron stripping process can, at least in principle, be calculated quantitatively using a direct reaction theory since all of the inputs are reasonably well known from other sources with the exception of the $^7\text{He} + ^{209}\text{Pb}$ exit channel optical potential. In Ref. [6] we performed such calculations using a few “physically reasonable” choices for the exit channel potential, fixing the other inputs—the entrance channel distorting potential and $\langle ^8\text{He} | ^7\text{He} + n \rangle$ and $\langle ^{209}\text{Pb} | ^{208}\text{Pb} + n \rangle$ overlaps—at values taken from the literature. The resulting cross sections accounted for about one third of the total ^6He cross section at 22 MeV, clearly a significant underestimate in the light of the kinematical considerations detailed in the preceding paragraph. We therefore performed new calculations in order to determine whether it was in fact possible to account for most of the ^6He cross section by the one-neutron stripping process while remaining within the bounds of what is physically acceptable with regard to the inputs.

The potentials binding the transferred neutron to the ^7He and ^{208}Pb cores were of standard Woods-Saxon form with radius and diffuseness parameters $r_0 = 1.25 \times A_{\text{core}}^{1/3}$ fm and $a = 0.65$ fm and the spectroscopic factors for the $\langle ^8\text{He} | ^7\text{He} + n \rangle$ and $\langle ^{209}\text{Pb} | ^{208}\text{Pb} + n \rangle$ overlaps were set to 4 and 1 respectively, the theoretical maximum values under the conventions used by the FRESKO code. The entrance channel distorting potential was as in Ref. [6]. The exit channel distorting potential remains an unknown since ^7He is unbound. In order to apply some physical constraints to the choice of this potential we calculated the real part using the double-folding procedure and a theoretical ^7He density [13]. This was then held fixed and the three parameters of the standard Woods-Saxon form imaginary potential varied to give the largest possible cross section. In the event, this was achieved with a so-called “interior” potential, the parameters being $W = 50$ MeV, $R_W = 1.0 \times 209^{1/3}$ fm, $a_W = 0.3$ fm. The result is plotted on Fig. 1(b) as the dashed curve.

We note here that, in contrast to the $2n$ -stripping calculations, the resulting angular distribution is sensitive to the choice of exit channel optical potential; cf. Fig. 4(b) of Ref. [6]. This is due to the kinematics of the reaction, since in the $1n$ -stripping case the energies of the ^7He ejectiles (before decaying into $^6\text{He} + n$) are relatively well above the relevant Coulomb barrier, unlike for the $2n$ stripping. While the choice of the imaginary part of the exit channel potential merely affects the height of the peak relative to the backward angle cross section, the peak position is sensitive to the choice of the real part, with shifts of up to 10° for a given imaginary potential. The calculation using the double-folded real potential based on the ^7He matter density of Ref. [13] gives the result closest to the measured ^6He angular distribution. Using a ^8He real potential, either double folded or the real part of the Woods-Saxon entrance potential, combined with the “interior” imaginary potential gives a similar result, the

peak cross section being shifted by approximately 2° to larger angles. Use of ${}^6\text{He}$, ${}^6\text{Li}$, or ${}^7\text{Li}$ real potentials as in Ref. [6] (but retaining the same “interior” imaginary potential referred to above) shifts the peak of the calculated angular distribution to even larger angles, by up to about 10° .

The measured inclusive ${}^6\text{He}$ angular distribution was fitted by summing the calculated one-neutron and two-neutron stripping cross sections together with a background function [denoted by the dot-dashed curve in Fig. 1(b)], the magnitudes of the two-neutron stripping and background being varied to give the best agreement with the data. The resulting sum is plotted in Fig. 1(b) as the solid curve, approximately 67% of the total (812 mb, cf. the experimental value of 871 ± 31 mb [6]) coming from one-neutron stripping, 16% from two-neutron stripping, and 17% from the background (including any contribution from breakup of ${}^8\text{He}$). An upper limit on the two-neutron stripping contribution is reasonably well defined by the measured backward angle ${}^6\text{He}$ cross section. The maximum value of the calculated $2n$ -stripping cross section consistent with this is about one third of the total, with essentially no contribution from the background. The lower limit on the two-neutron stripping contribution is about 12% of the total, this being the minimum consistent with a good description of the measured ${}^6\text{He}$ angular distribution, with a corresponding increase in the background contribution. Assessing the uncertainty on the $1n$ -stripping contribution is more difficult, but any variation greater than about $\pm 10\%$ would lead to a significant degradation of the description of the ${}^6\text{He}$ angular distribution.

We therefore conclude that the measured inclusive ${}^6\text{He}$ angular distribution for the interaction of a 22 MeV ${}^8\text{He}$ beam with a ${}^{208}\text{Pb}$ target is indeed consistent with one-neutron stripping as the dominant ${}^6\text{He}$ production mechanism, with two-neutron stripping playing a minor role, contributing at most about one third of the total. This has important implications for the ${}^4\text{He}$ production mechanism which we address in the following section.

B. Analysis of the ${}^4\text{He}$ yield

We now turn to a detailed consideration of the ${}^4\text{He}$ production. In addition to neutron transfer processes the measured inclusive ${}^4\text{He}$ angular distribution will contain any contribution from breakup of the ${}^8\text{He}$ projectile, as in the ${}^6\text{He}$ case, but may also include α particles arising from fusion-evaporation events. In our analysis of the inclusive ${}^4\text{He}$ production cross section these latter two processes are subsumed into the background since they are expected to be small compared to the transfer yield.

The following neutron transfer processes could contribute to the inclusive ${}^4\text{He}$ yield (we do not consider transfers with more than two steps):

- (1) ${}^{208}\text{Pb}({}^8\text{He}, {}^4\text{He}){}^{212}\text{Pb}$.
- (2) ${}^{208}\text{Pb}({}^8\text{He}, {}^5\text{He} \rightarrow {}^4\text{He} + n){}^{211}\text{Pb}$.
- (3) ${}^{208}\text{Pb}({}^8\text{He}, {}^6\text{He}^* \rightarrow {}^4\text{He} + 2n){}^{210}\text{Pb}$.
- (4) ${}^{208}\text{Pb}({}^8\text{He}, {}^6\text{He}){}^{210}\text{Pb}({}^6\text{He}, {}^4\text{He}){}^{212}\text{Pb}$.
- (5) ${}^{208}\text{Pb}({}^8\text{He}, {}^7\text{He}^* \rightarrow ({}^6\text{He}^* \rightarrow {}^4\text{He} + 2n) + n){}^{209}\text{Pb}$.
- (6) ${}^{208}\text{Pb}({}^8\text{He}, {}^7\text{He}){}^{209}\text{Pb}({}^7\text{He}, {}^6\text{He}^* \rightarrow {}^4\text{He} + 2n){}^{210}\text{Pb}$.
- (7) ${}^{208}\text{Pb}({}^8\text{He}, {}^7\text{He}){}^{209}\text{Pb}({}^7\text{He}, {}^4\text{He}){}^{212}\text{Pb}$.

We may immediately rule out any significant contribution from process 4, the sequential transfer of two $2n$ clusters, since we have shown in the previous section that the initial step must have a small cross section on purely kinematic grounds. Processes 6 and 7 at first sight appear possible significant contributors due to the strong population of the intermediate step, as demonstrated in the previous section. However, they may be ruled out on structural grounds: In process 6 the intermediate step populates low-lying single particle levels in ${}^{209}\text{Pb}$ below 4 MeV in excitation energy which are unlikely to have significant overlap with levels in ${}^{210}\text{Pb}$ in the required excitation energy range, around 8 MeV or so. For process 7 to contribute significantly the second step would require a significant overlap between the ground state of ${}^7\text{He}$ and the $\alpha + 3n$ configuration, which seems unlikely given the accepted status of ${}^7\text{He}$ as a ${}^6\text{He} + n$ resonance (see, e.g., Ref. [14]). Process 5 is unlikely since there appears to be little overlap between the ground state of ${}^8\text{He}$ and excited states of ${}^7\text{He}$; see, e.g., the ${}^8\text{He}(p, d)$ work of Ref. [12], and in any case the known levels are broad, with widths of a few MeV [15]. Process 3 also seems unlikely since the overlap between the ground state of ${}^8\text{He}$ and at least the 1.8 MeV 2^+ excited state of ${}^6\text{He}$ is small [12], although this need not necessarily be the case for the other known low-lying levels of ${}^6\text{He}$ at 2.6 and 5.3 MeV [16]. However, test calculations of $2n$ stripping populating these levels in ${}^6\text{He}$ found that not only was the cross section significantly smaller than for populating the ground state (even with the same spectroscopic factor) but the angular distributions peaked at larger angles as the excitation energy of the ${}^6\text{He}$ resonance increased, moving the peak of the corresponding ${}^4\text{He}$ distribution further away from the peak of the observed inclusive ${}^4\text{He}$ angular distribution. Finally, process 2 does not seem a likely candidate since it would require a sizable overlap between the ground state of ${}^8\text{He}$ and the ${}^5\text{He} + 3n$ configuration in order to make a significant contribution, and we are not aware of any structure calculations that explicitly mention significant $3n$ clustering in the ground state of ${}^8\text{He}$.

We are thus left with process 1, direct $4n$ stripping, as our candidate main mechanism for production of ${}^4\text{He}$. Transfer of four neutrons can in principle populate states in ${}^{212}\text{Pb}$ from the ground state ($Q = +14.99$ MeV) up to the four-neutron separation energy at $E_x = 18.08$ MeV ($Q = -3.11$ MeV), or even beyond if resonant-like states are considered. However, as discussed in Ref. [6], the optimum Q value for this process is $Q = -1.7$ MeV so that final states around 16.7 MeV in excitation energy are expected to be preferentially populated. A consideration of the observed two-dimensional ${}^4\text{He}$ total energy versus scattering angle spectrum together with the kinematics of the ${}^{208}\text{Pb}({}^8\text{He}, {}^4\text{He}){}^{212}\text{Pb}$ reaction, assumed to be direct $4n$ transfer, enables us to fix the range of allowed excitation energies of the residual ${}^{212}\text{Pb}$ nucleus. Under this assumption only states in ${}^{212}\text{Pb}$ with $14 \leq E_x \leq 22$ MeV can be populated, see Fig. 2(a).

To test whether such a process, subject to these kinematic constraints, can reproduce the shape of the measured inclusive ${}^4\text{He}$ angular distribution, DWBA calculations were performed for direct $4n$ transfer to states in ${}^{212}\text{Pb}$ at excitation energies of 14, 16, 18, 20, and 22 MeV, covering the observed energy

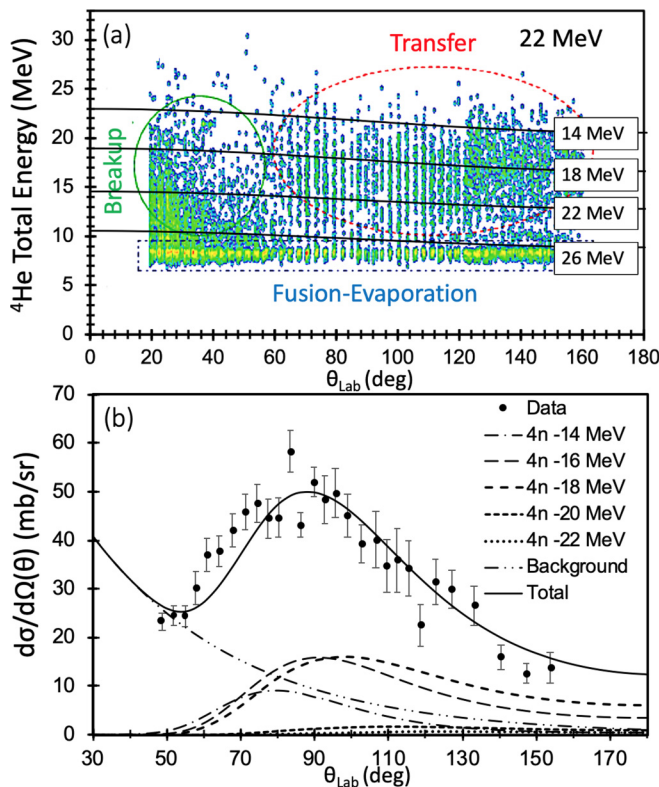


FIG. 2. (a) Experimental ^4He total energy versus scattering angle two-dimensional spectrum for 22 MeV ^8He incident on a ^{208}Pb target. Superimposed are kinematic curves for ^4He ejectiles produced by the $^{208}\text{Pb}(^8\text{He}, ^4\text{He})^{212}\text{Pb}$ $4n$ -stripping reaction with the ^{212}Pb residual in states with $E_x = 14, 18, 22,$ and 26 MeV (reading from the top down). (b) Angular distribution of the inclusive ^4He production for 22 MeV ^8He incident on a ^{208}Pb target. The filled circles denote the data of Ref. [6]. The various styles of broken curve denote the results of DWBA calculations of direct $4n$ transfer to states in ^{212}Pb at the labeled excitation energies and the background. The solid curve denotes the total (sum of all transfer calculations plus background). See text for details.

range of ^4He recoils, with angular momentum $L = 6\hbar$ relative to the ^{208}Pb core, approximately the best matched L value. The shape of the angular distribution is only weakly dependent on the value of L . The potentials binding the $4n$ cluster to the ^4He and ^{208}Pb cores were of Woods-Saxon form with parameters $r_0 = 1.0 \times (4 + A_{\text{core}}^{1/3})$ fm and $a = 0.65$ fm. The spin-parity of the $4n$ cluster was assumed to be 0^+ , the simplest possibility consistent with the presence of such a cluster in the ground state of ^8He . The optical potential in the entrance channel was the same as in the previous section. The $^4\text{He} + ^{208}\text{Pb}$ optical potential parameters of Ref. [17] were used in the exit channel. Since the calculations were purely qualitative all spectroscopic factors were set equal to 1.0. The form factors for the states at $E_x = 20$ and 22 MeV were calculated assuming nominal binding energies of 0.01 MeV for the $4n$ cluster with respect to the ^{208}Pb core since these values of E_x are above the $4n$ emission threshold of ^{212}Pb .

The inclusive ^4He angular distribution for 22 MeV ^8He incident on a ^{208}Pb target of Ref. [6] was fitted by adjusting the

normalizations of the DWBA curves and the parameters of an exponential background function (including any contributions from breakup of the ^8He projectile and fusion-evaporation) to give the best description of the data. The data were obtained by integrating, for each laboratory scattering angle, the energy distribution above the 8.78 MeV alpha peak arising from the decay of the ^{212}Po ground state. To assist in fixing the parameters of the background function the angular range of the data was slightly extended to more forward angles than in Ref. [6]. Care was also taken to avoid unrealistically large contributions from the calculations with E_x values at the limits of the kinematically allowed range. The results of this analysis are displayed in Fig. 2(b). As in the case of the $2n$ cluster transfer, the calculated shapes of the angular distributions were not very sensitive to the transferred angular momentum but did depend on the excitation energy of the recoil ^{212}Pb nucleus; see Fig. 2(b).

Our results suggest that the ^4He yield can be well described by a combination of direct $4n$ transfer and an exponential background function, the transfer accounting for 73% of the total (355 mb, cf. the experimental value of 393_{-33}^{+10} mb [6]).

III. SUMMARY AND CONCLUSIONS

In a previous article [6] analyzing the measured inclusive ^6He and ^4He yields for the $^8\text{He} + ^{208}\text{Pb}$ system we concluded, with the aid of DWBA calculations, that for an incident ^8He energy of 22 MeV the $^{208}\text{Pb}(^8\text{He}, ^7\text{He})^{209}\text{Pb}$ single-neutron stripping reaction was responsible for about one third of the total measured ^6He cross section, the remaining two thirds being mainly due to the $^{208}\text{Pb}(^8\text{He}, ^6\text{He})^{210}\text{Pb}$ two-neutron stripping since kinematic considerations ruled out breakup as a significant contributor over the measured angular range. In this work we have revised this conclusion in favor of the single-neutron stripping mechanism, since a detailed consideration of the kinematics of the two-neutron stripping reaction in conjunction with the experimental ^6He total energy versus scattering angle spectrum places strict limits on the range of possible excitation energies of the ^{210}Pb residual which, when applied to DWBA calculations, exclude the possibility of the $2n$ -stripping providing the main contribution to the measured inclusive ^6He angular distribution.

The relatively small contribution to the inclusive ^6He yield from two-neutron stripping—estimated to be at most about 30%—is a robust result, since it is mainly based on kinematics. Distorted wave Born approximation calculations of the $2n$ -stripping reaction were unable to reproduce the shape of the measured ^6He angular distribution while remaining within the kinematically allowed values of the ^{210}Pb excitation energy, independently of the choice of input parameters, the calculated angular distributions being essentially insensitive to the exit channel potential due to the low energies of the ^6He ejectiles relative to the respective Coulomb barrier. It was further demonstrated that the remainder of the measured inclusive ^6He yield can be explained as mostly arising from the single-neutron stripping reaction—approximately 70% of the total—plus a small exponential background representing the contribution of breakup. However, the DWBA calculations of the single-neutron stripping are more sensitive to

the choice of exit channel optical potential, the energies of the ${}^7\text{He}$ ejectiles (before decaying into ${}^6\text{He} + n$) being above the respective Coulomb barrier, and a good description of the ${}^6\text{He}$ yield is dependent on the use of a particular potential. Since ${}^7\text{He}$ is unbound it is impossible to check whether this potential is consistent with the appropriate elastic scattering, although it is at least physically reasonable.

Based partly on these results, but also on additional kinematic and structural considerations, it was further argued that the inclusive ${}^4\text{He}$ production was most likely dominated by direct $4n$ transfer. This conclusion was borne out by DWBA calculations assuming only the ${}^{208}\text{Pb}({}^8\text{He}, {}^4\text{He}){}^{212}\text{Pb}$ direct $4n$ transfer mechanism which, combined with a small background contribution, were able to describe very well the measured inclusive ${}^4\text{He}$ angular distribution of Ref. [6]. These results are consistent with the direct $4n$ transfer channel suggested in Ref. [3]. This picture is also appealing in view of the strong beta-decay triton branch of ${}^8\text{He}$ [18,19], which could originate from the decay of the four-neutron skin. This process would be the four-neutron equivalent to the deuteron decay branch observed in ${}^{11}\text{Li}$ [20]. However, this conclusion is less robust than that concerning the ${}^6\text{He}$ production since at present nothing is known of the structure of ${}^{212}\text{Pb}$ in the

excitation energy region preferentially populated by the $4n$ stripping reaction, so that the DWBA calculations remain purely qualitative.

The relative unimportance of $2n$ stripping does not necessarily contradict the possibility of a significant dineutron condensate component in the ground state of ${}^8\text{He}$, as suggested by recent theoretical predictions obtained from Hartree-Fock-Bogoliubov calculations [21] and the alpha-dineutron condensate method [22]. The cross sections of direct reactions are strongly dependent on kinematic matching conditions (Q value and angular momentum transfer) as well as the structure of the nuclei involved so that different aspects of the structure may be emphasized by different reactions. Both the Q matching conditions and structure considerations combine in this particular case to favor the $({}^8\text{He} | {}^7\text{He} + n)$ and, to a lesser extent, the $({}^8\text{He} | {}^4\text{He} + 4n)$ components of the ${}^8\text{He}$ ground state.

ACKNOWLEDGMENTS

This work was supported by the Ministry of Science and Higher Education of Poland, Grant No. N202033637, and by the Ministry of Science, Innovation and Universities of Spain, Grant No. PGC2018-095640-B-I00.

-
- [1] M. V. Zhukov, B. V. Danilin, D. V. Fedorov, J. M. Bang, I. J. Thompson, and J. S. Vaagen, *Phys. Rep.* **231**, 151 (1993).
- [2] G. M. Ter-Akopian, A. M. Rodin, A. S. Fomichev, S. I. Sidorchuk, S. V. Stepantsov, R. Wolski *et al.*, *Phys. Lett. B* **426**, 251 (1998).
- [3] R. E. Tribble, J. D. Cossairt, K. I. Kubo, and D. P. May, *Phys. Rev. Lett.* **40**, 13 (1978).
- [4] R. Wolski, S. I. Sidorchuk, G. M. Ter-Akopian, A. S. Fomichev, A. M. Rodin, S. V. Stepantsov *et al.*, *Nucl. Phys. A* **722**, 55c (2003).
- [5] A. Lemasson, A. Navin, N. Keeley, M. Rejmund, S. Bhattacharyya, A. Shrivastava *et al.*, *Phys. Rev. C* **82**, 044617 (2010).
- [6] G. Marquínez-Durán, I. Martel, A. M. Sánchez-Benítez, L. Acosta, J. L. Aguado, R. Berjillos *et al.*, *Phys. Rev. C* **98**, 034615 (2018).
- [7] M. V. Zhukov, A. A. Korshennikov, and M. H. Smedberg, *Phys. Rev. C* **50**, R1 (1994).
- [8] G. Marquínez-Durán, L. Acosta, R. Berjillos, J. A. Dueñas, J. A. Labrador, K. Rusek, A. M. Sánchez-Benítez, and I. Martel, *Nucl. Instrum. Methods Phys. Res., Sect. A* **755**, 69 (2014).
- [9] G. Marquínez-Durán, I. Martel, A. M. Sánchez-Benítez, L. Acosta, R. Berjillos, J. Dueñas, K. Rusek, N. Keeley, M. A. G. Álvarez, M. J. G. Borge *et al.*, *Phys. Rev. C* **94**, 064618 (2016).
- [10] I. J. Thompson, *Comput. Phys. Rep.* **7**, 167 (1988).
- [11] A. M. Sánchez-Benítez, D. Escrig, M. A. G. Álvarez, M. V. Andrés, C. Angulo, M. J. G. Borge *et al.*, *Nucl. Phys. A* **803**, 30 (2008).
- [12] N. Keeley, F. Skaza, V. Lapoux, N. Alamanos, F. Auger, D. Beaumel *et al.*, *Phys. Lett. B* **646**, 222 (2007).
- [13] T. Neff and H. Feldmeier, *Nucl. Phys. A* **738**, 357 (2004).
- [14] Yu. Aksyutina, T. Aumann, K. Boretzky, M. J. G. Borge, C. Caesar, A. Chatillon *et al.*, *Phys. Lett. B* **718**, 1309 (2013).
- [15] K. Fossez, J. Rotureau, and W. Nazarewicz, *Phys. Rev. C* **98**, 061302(R) (2018).
- [16] X. Mougeot, V. Lapoux, W. Mittig, N. Alamanos, F. Auger, B. Avez *et al.*, *Phys. Lett. B* **718**, 441 (2012).
- [17] G. M. Hudson and R. H. Davis, *Phys. Rev. C* **9**, 1521 (1974).
- [18] M. J. G. Borge, M. Epherre-Rey-Campagnolle, D. Guillemaud-Mueller, B. Jonson, M. Langevin, G. Nyman, C. Thibault, and The ISOLDE Collaboration, *Nucl. Phys. A* **460**, 373 (1986).
- [19] M. J. G. Borge, L. Johannsen, B. Jonson, T. Nilsson, G. Nyman, K. Riisager, O. Tengblad, K. Wilhelmsen-Rolander, and The ISOLDE Collaboration, *Nucl. Phys. A* **560**, 664 (1993).
- [20] R. Raabe, A. Andreyev, M. J. G. Borge, L. Buchmann, P. Capel, H. O. U. Fynbo *et al.*, *Phys. Rev. Lett.* **101**, 212501 (2008).
- [21] K. Hagino, N. Takahashi, and H. Sagawa, *Phys. Rev. C* **77**, 054317 (2008).
- [22] F. Kobayashi and Y. Kanada-En'yo, *Phys. Rev. C* **88**, 034321 (2013).